Octanuclear manganese(II,III) clusters stabilized with diamino-alcoxo ligands†

Albert Escuer,*[a] Ramon Vicente,[a] M. Salah El Fallah,[a] E. Carolina Sañudo,[a] Simon J. Teat,‡[b] Fabrizia Fabrizi de Biani[c] and Piero Zanello[c]

Received 12th May 2009, Accepted 21st September 2009
First published as an Advance Article on the web 16th October 2009
DOI: 10.1039/b909371k

The employment of the 1,3-bis(dimethylamino)-2-propanolate (bdmap) ligand as a chelating/bridging ligand in manganese chemistry is described. The reaction of Mn(R-BzO)$_2$ and bdmap affords [Mn$_8$(O)$_4$(R-BzO)$_{12}$(bdmap)$_2$(H$_2$O)$_2$], R = H (**1**), R = 3-Cl (**2**) and R = 4-Cl (**3**), which are mixed-valence Mn$^{II}_2$Mn$^{III}_6$ clusters. Structural characterization was achieved for **1** and **2**, which can be described as a central double defective dicubane Mn$^{III}_4$ subunit, capped by two oxo-bridged Mn^{II}-μ(bdmap)-Mn^{III} dinuclear units. DC variable-temperature magnetic susceptibility studies were carried out in the 2–300 K range, revealing an overall antiferromagnetic behaviour for **1–3**. This work demonstrates for the first time the ability of this kind of polytopic ligands in high nuclearity manganese chemistry.

Introduction

The search for new single molecule magnets (SMMs) and the study of their magnetic properties has been one of the areas of transition metal chemistry that has attracted more attention in the last few years.[1] The development of new synthetic strategies that can yield high nuclearity systems is one of the current active research fields in molecular magnetism. This largely relies in the choice of new ligands or reaction systems that will potentially afford high nuclearity coordination complexes. A large variety of ligands containing at least one deprotonated O-donor atom (hydroxo, alcoxo, oximato, *etc.*), have been successfully employed in the synthesis of new clusters. This kind of O-donor have the ability to bridge up to three metallic ions and to build large polymetallic arrays. One of the common strategies is to choose polytopic ligands, in which good donors such as amino or pyridyl N-atoms aid in the coordination of the ligand whereas one or more oxo-containing arms target the increase of the nuclearity of the resulting polymetallic compounds. During the last few years monoaminodiol or–triol ligands (Scheme 1a) or pyridine-2,6-dimethanol (Scheme 1b) have been used[2] to generate high nuclearity manganese systems as impressive as Mn$_{19}$,[3] Mn$_{25}$,[4] Mn$_{32}$[5] clusters or dodecamanganese[6] wheels, in which simultaneous coordination of the N-amino donor and the two or three O-alcoxo atoms was found. Ligands with more than one N-donor atom and one or two alcoxo groups like the well known *gem*-diol derived from di-2-pyridyl ketone (Scheme 1c) have also been used with success in the syntheses of high-nuclearity clusters.[2] In contrast, the chemistry of diaminoalcoxo ligands as may be 1,3-bis-amino-2-propanolate (bdap) and 1,3-bis(dimethylamino)-2-propanolate (bdmap) ligands, Scheme 1d, which are potentially good polynucleating ligands, remains practically unexplored: only one tetranuclear[7] bdap/azido and one heptanuclear[8] bdap/nitrito nickel systems were reported in the 90's. More recently, we have explored the coordination properties of bdap and bdmap ligands, obtaining a number of Cu$_4$, Cu$_6$, Cu$_8$, Cu$_9$ or *n*-D derivatives.[9] Following with our work with these ligands we have studied the reactivity of bdmap with several manganese carboxylates. Starting from benzoate or substituted benzoate salts, octanuclear Mn$^{II}_2$Mn$^{III}_6$ complexes with general formula [Mn$_8$(O)$_4$(R-BzO)$_{12}$(bdmap)$_2$(H$_2$O)$_2$], R = H (**1**), R = 3-Cl (**2**) and R = 4-Cl (**3**) were obtained and characterized. This work shows that this kind of ligands can easily stabilize Mn^{II}/Mn^{III} systems in contrast with polydentate amines, which typically fail to yield stable manganese complexes in aerobic/oxidant conditions.

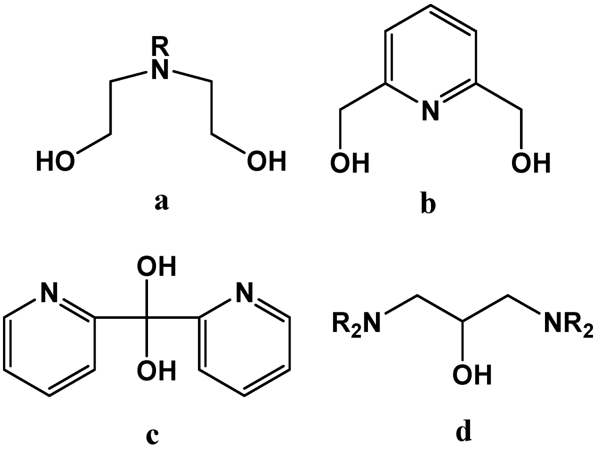

Scheme 1 Some typical polynucleating ligands with N/O donors.

---

[a] *Departament de Química Inorgànica and Institut de Nanociencia i Nanotecnologia de la Universitat de Barcelona (IN^{2}UB), Martí Franqués 1-11, 08028, Barcelona, Spain. E-mail: albert.escuer@qi.ub.es; Fax: +34 93490 7725*
[b] *CLRC Daresbury Laboratory, Daresbury, Warrington, Cheshire, UK WA4 4AD*
[c] *Dipartimento di Chimica dell'Università di Siena, Via A. De Gasperi, 2, I-53100, Siena, Italy*

† CCDC reference numbers 648710 and 648711. For crystallographic data in CIF or other electronic format see DOI: 10.1039/b909371k

‡ Present address: Advance Light Source, Lawrence Berkeley Laboratory, 1 Cyclotron Road, Berkeley, California, 94720, USA

Experimental

Syntheses

$[Mn_8(O)_4(BzO)_{12}(bdmap)_2(H_2O)_2]$ (**1**). The air oxidation of a stirred methanolic solution of 1 mmol (0.369 g) of manganese benzoate tetrahydrate and 1 mmol (0.146 g) of 1,3-bis-(dimethylamino)-2-propanol gives a dark red solution in one hour. After removal of the solvent, a brown solid was obtained which was dissolved in dichloromethane and layered with hexanes. Well formed, small, dark red crystals, were obtained after two days in a 60% yield.

Compounds **2** and **3** in similar yield were obtained by using 3-Cl- or 4-Cl-benzoate salts, respectively, and following the same procedure.

The dried solids were analyzed as solvent free. **1**, Anal. calcd for $C_{98}H_{98}Mn_8N_4O_{32}$: C 51.6, H 4.3, N 2.4. Found: C 50.8, H 4.4, N 2.3%. **2**, Anal. calcd for $C_{98}H_{86}Mn_8N_4O_{32}Cl_{12}$: C 43.7, H 3.2, N 2.1. Found: C 43.9, H 3.10, N 2.2%. **3**, Anal. calcd for $C_{98}H_{86}Mn_8N_4O_{32}Cl_{12}$: C 43.7, H 3.2, N 2.1. Found: C 43.3, H 3.0, N 2.3%.

Reaction in the same conditions of other carboxylates (acetate, formate) with bdmap or benzoates with bdap gives also red solutions by air oxidation but crystalline compounds were not obtained.

X-Ray structure determination

$[Mn_8(O)_4(BzO)_{12}(bdmap)_2(H_2O)_2]$ (**1**). Data were collected on a OXFORD Diffraction Xcalibur 2 diffractometer. Several crystals were tried, and the best dataset was refined. The crystals lost solvent very fast and diffracted poorly, thus data were collected at low temperature and only to 23.3°. The asymmetric unit contains one half of Mn_8 cluster. The $C_7H_{17}N_2O$ ligand was disordered and modelled over two sites. The atoms O71 and O71a, corresponding to the disordered ligand were kept isotropic. Hydrogen atoms were calculated riding on their respective C and fixed and kept isotropic. Two molecules of heavily disordered CH_2Cl_2 and 1/2 MeOH per Mn_8 cluster were removed using the Squeeze option in Platon to obtain an improved 'difference-map'.[10] The structure was solved by direct methods using the program SHELXS-97[11] and refined by full-matrix least-squares methods against F^2 with SHELXL-97.[11]

$[Mn_8(O)_4(3Cl\text{-}BzO)_{12}(bdmap)_2(H_2O)_2]$ (**2**). Data were collected using a Bruker APEX II CCD diffractometer on station 9.8 of the Synchrotron Radiation Source at CCLRC Daresbury Laboratory, at 0.6894 Å, from a silicon(111) monochromator. All non-hydrogens were refined anisotropically except for those that are not fully occupied, that is, the atoms of the $C_7H_{17}N_2O$ ligand. Displacement and geometrical restrains were used in modelling the disordered solvent molecules and the disordered ligand. H-atoms were placed geometrically and refined using a riding model. The hydrogens on the water molecule O(3) could not be found in the difference map or placed geometrically and were therefore omitted from the refinement. Several of the chlorines have anisotropic displacement ratios of around 4 : 1 (max : min) while this is not ideal it does reflect the motion of the molecule and therefore they were left as they are. Crystal data and parameters for data collection are listed in Table 1.

Table 1 Summary of crystal data, data collection and structure refinement for compounds **1–2**

	$\mathbf{1}\cdot 2CH_2Cl_2\cdot 1/2MeOH$	$\mathbf{2}\cdot 4CH_2Cl_2$
Empirical formula	$C_{98}H_{98}Mn_8N_4O_{32}$	$C_{98}H_{98}Cl_{12}Mn_8N_4O_{32}$
Formula weight	2469.22	3036.40
λ/Å	0.71073	Synchrotron, 0.68940
T/K	100(2)	150(2)
θ range/°	2.7–23.3	1.9–29.50
Crystal system; space group	Trigonal; $R\bar{3}$	Triclinic, $P\bar{1}$
Crystal dimensions/mm^3	0.06 x 0.17 x 0.17	0.06 × 0.06 × 0.04
a/Å	36.159(3)	14.655(2)
b/Å	36.159(3)	14.977(2)
c/Å	24.384(2)	15.039(2)
α/°	90	75.010(2)
β/°	90	78.017(2)
γ/°	120	69.914(2)
V/Å^3	27 610(4)	2968.8(6)
Z	9	1
D_{calcd}/g cm^{-3}	1.234	1.698
μ/mm^{-1}	0.863	1.350
Reflections collected/unique	53 077/8841	34 409/17599
Parameters	720	781
R_{int}	0.18	0.045
Final R indices [$I > 2\sigma(I)$]	0.0699	0.0636
R indices (all data)	0.2075	0.1930
Largest diffraction peak and hole/e Å^{-3}	–0.70, 1.35	–1.30 and 1.36

Physical measurements

Magnetic susceptibility measurements were carried out on polycrystalline samples with a Quantum Design DSM5 susceptometer working in the range 2–300 K under magnetic fields of 0.3 T and re-measured under a field of 0.03 T in the 20–2 K range to discard saturation effects. Diamagnetic corrections were estimated from Pascal Tables. Infrared spectra (4000–200 cm^{-1}) were recorded from KBr pellets on a Bruker IFS-125 FT-IR spectrophotometer.

Results and discussion

Description of the structures

Structural data were obtained for $[Mn_8(O)_4(R\text{-}BzO)_{12}(bdmap)_2(H_2O)_2]$ (R = H (**1**), 3-Cl (**2**)). Both species possessed the same core, only differing in the R group attached to the aromatic ring. Structural discussion will be focused on **2** assuming that its description is fully applicable to **1**. Selected bond parameters for **2** are listed in Table 2.

$[Mn_8(O)_4(3\text{-}ClBzO)_{12}(bdmap)_2(H_2O)_2]\cdot 2CH_2Cl_2\cdot 1/2MeOH$ (2).

Each octanuclear neutral unit sits in a crystallographic inversion centre. It can be described as a central double defective dicubane $Mn^{III}{}_4$ subunit with the four manganese atoms in the same plane, capped by two oxo-bridged Mn^{II}-μ(bdmap)-Mn^{III} dinuclear units, Fig. 1. The oxidation state of the manganese atoms can be deduced from the stoichiometry of the compound and the bond distances around the cations: Mn(1), Mn(2) and Mn(3) exhibits four short bond distances, with values lower than 2 Å and axially elongated

Table 2 Bond distances around the manganese atoms and selected bond angles for compound **2**

Bond distances/Å			
Mn(1)–O(2)	1.883(2)	Mn(3)–O(1)	1.887(2)
Mn(1)–O(21′)	1.929(2)	Mn(3)–O(51)	2.243(2)
Mn(1)–O(52)	1.946(2)	Mn(3)–O(71)	1.921(3)
Mn(1)–O(1)	1.880(2)	Mn(3)–O(31)	2.179(2)
Mn(1)–O(11′)	2.174(3)	Mn(3)–O(61)	1.906(3)
Mn(1)–O(42′)	2.475(3)	Mn(3)–N(71)	2.100(3)
Mn(2)–O(1)	1.855(2)	Mn(4)–O(2′)	2.138(2)
Mn(2)–O(2′)	2.254(2)	Mn(4)–O(22)	2.164(2)
Mn(2)–O(32)	1.954(2)	Mn(4)–N(72)	2.316(3)
Mn(2)–O(2)	1.897(2)	Mn(4)–O(12)	2.165(3)
Mn(2)–O(3)	2.248(3)	Mn(4)–O(41′)	2.227(2)
Mn(2)–O(42)	1.966(2)	Mn(4)–O(71)	2.210(3)
Bond angles/°			
Mn(1)–O(1)–Mn(2)	98.8(1)	Mn(2)–O(1)–Mn(3)	130.8(1)
Mn(1)–O(1)–Mn(3)	130.3(1)	Mn(2)–O(2)–Mn(2′)	96.41(9)
Mn(1)–O(2)–Mn(2)	97.3(1)	Mn(2)–O(2)–Mn(4′)	121.4(1)
Mn(1)–O(2)–Mn(2′)	104.2(1)	Mn(2′)–O(2)–Mn(4′)	114.8(1)
Mn(1)–O(2)–Mn(4′)	119.0(1)	Mn(3)–O(71)–Mn(4)	134.8(1)
Mn(1′)–O(42)–Mn(2)	94.22(9)		

distances comprised between 2.174 and 2.475 Å, indicating clearly the Mn^{III} oxidation state. In contrast, Mn(4) exhibits six larger bond lengths comprised between 2.138 and 2.316 Å, typically associated to Mn^{II}. Then, structural data confirms unambiguously the $Mn_2^{II}Mn_6^{III}$ formula. The core of the cluster consists of eight Mn atoms linked by oxo bridging ligands: one alcoxo bridge between Mn(3) and Mn(4) by means of O(71) (from the two bdmap ligands), O(1) μ_3-oxo bridges between Mn(1), Mn(2) and Mn(3), O(2) μ_4-oxo bridges between Mn(1), Mn(2), Mn(2′) and Mn(4′) and the O(42) oxygen atoms from two of the carboxylates which gives μ_2-oxo bridges between Mn(1′) with Mn(2). In addition, eight of the twelve carboxylates act as a bridge between the manganese atoms in the common *syn–syn* coordination mode and the two remaining carboxylates act as a monodentate ligand on Mn(3) and the symmetry related Mn(3)', linked by O(62)···O(3) H-bonds (2.725 Å) to the water molecule coordinated to Mn(2). The Mn(3)–O(71)–Mn(4) bond angle takes a value of 134.8(1)°. The small values for the bond angles Mn(1)–O(1)–Mn(2) and Mn(1)–O(2)–Mn(2) of 98.8(1)° and 97.3(1)°, respectively, gives a short Mn(1)···Mn(2) distance of 2.8365(7) Å. Eight of the benzoate groups are placed in four pairs of parallel rings stabilized by π–π interactions (distance between centroids around 3.6 Å), Fig. 1.

The structure of these compounds is related with that reported by Christou *et al.*[12] for $(NB^n{}_4)_2$ $[Mn_8O_4(O_2CPh)_{12}(Et_2mal)_2(H_2O)_2]$ Et_2mal = diethyl-malonato (**4**), which features the same $Mn_2^{II}Mn_6^{III}$ core, with similar bond distances and angles. It should be emphasised that these structures are very close despite the different charge of the cluster and the different origin of the Mn^{II}–O–Mn^{III} bond, from an alcoxo ligand (bdmap) in **1–2** or from one of the carboxylates of the malonato ligands in **4**, Fig. 2.

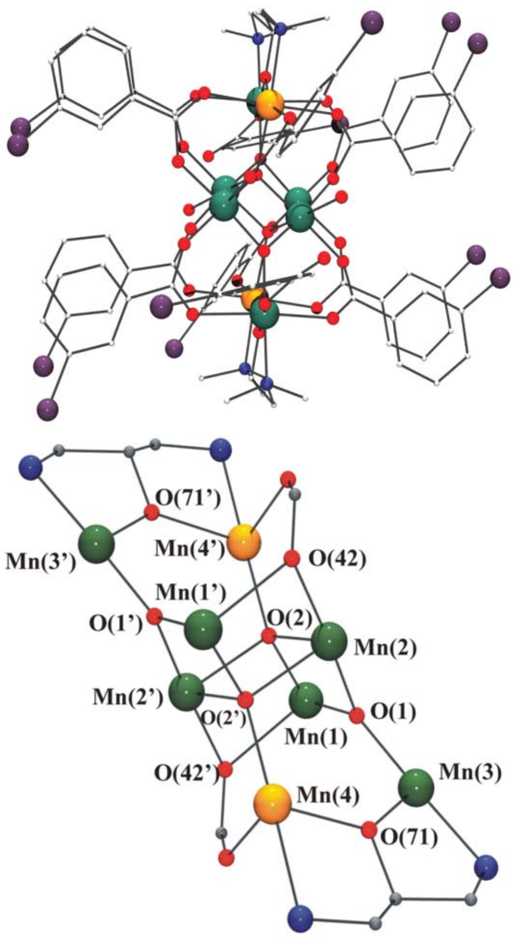

Fig. 1 Top, plot of the structure of **2** showing the octanuclear cluster and the π–π interactions between the aromatic rings. Bottom, labelled core of the cluster, showing the coordination of the bdmap ligands. (Mn^{III} green, Mn^{II} yellow, O red, N blue, Cl violet). Axial elongation for the trivalent manganese atoms follows the Mn(1)–O(42′) and Mn(2)–O(2′) directions. Hydrogen atoms and solvent molecules are not shown for clarity.

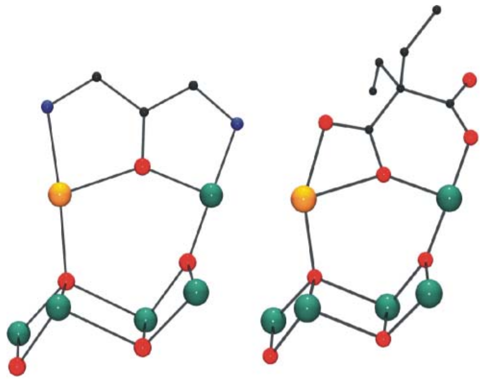

Fig. 2 Partial view of the core of compounds **1–2** (left, bdmap bridging ligand) and **4** (right, Et_2mal bridging ligand).

Electrochemistry

In view of the multi-valent nature of complexes **1–2**, their redox aptitude has been studied. Both complexes give rise to cyclic voltammetric responses rather ill shaped, probably because of electrode poisoning phenomena, which by no way could be avoided by changing the experimental conditions. The best results have been obtained for **1** in dichloromethane solution using a platinum working electrode. The pertinent cyclic (CV) and differential pulse (DPV) voltammograms are shown in Fig. 3.

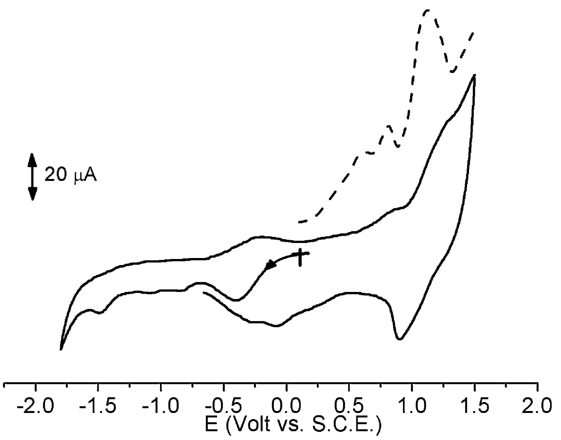

Fig. 3 Cyclic (—) and differential pulse (---) voltammetric responses recorded at platinum electrode in CH_2Cl_2 solution containing **1** (0.3×10^{-3} mol dm^{-3}). $[NBu_4][PF_6]$ (0.2 mol dm^{-3}) supporting electrolyte. Scan rate 0.2 V s^{-1}.

Either a reduction ($E^{\circ\prime} = -0.31$ V; $\Delta E_p = 170$ mV, $ip_a/ip_c = 0.6$ at 0.2 V s^{-1}) or an oxidation ($E^{\circ\prime} = +1.12$ V; $\Delta E_p = 380$ mV, $ip_c/ip_a = 0.9$ at 0.2 V s^{-1}) are clearly detected in the cyclic voltammogram.

Both processes have features of partial chemical reversibility. In fact, a series of spurious signals are detected in the respective back scans, thus suggesting the formation of byproducts either upon oxidation or reduction. It is, however, noted that the DPV profile also puts in evidence the presence of two further oxidations processes at $E_p = +0.63$ V and +0.82 V, respectively. Because of the poisoning effects, any attempt to determine the number of electrons involved in such processes by controlled potential coulometry failed. On the basis of the peak–current ratio and of the compound stoichiometry, one could assume that the first less intense oxidation might be ascribed to the Mn^{II}/Mn^{III} redox change of the two Mn^{II} centres, followed by chemical complications which are responsible for the appearance of the second minor signal (even if it cannot be ruled out that the two minor oxidations might be due to the separate oxidation of the two Mn^{II} centres). In turn, the third, more intense, oxidation might be attributed to the concomitant Mn^{III}/Mn^{IV} redox change of the four Mn^{III} ions, which are in an octahedral environment. The reduction process is presumably due to the Mn^{III}/Mn^{II} redox change of the pentacoordinated Mn^{III} ions, which, in fact, are expected to be easier to reduce and more difficult to oxidise than those in an octahedral environment. Unfortunately, it resulted impossible to obtain adequately shaped cyclic voltammograms for compound **2**. Anyway, exploiting the aptitude of **2** to poison the electrode surface, we have been able to obtain electrodeposition of a thin film of **2** by repeatedly cycling its CH_2Cl_2 solution at an ITO electrode from +1.5 V to −1.8 V, Fig.4. It is noteworthy that once formed, the film of **2** displays a redox profile similar to that observed for **1** in solution. The use of the **2**/ITO modified electrode in a blank solution confirms the stability of the film, at least for a few tenth of cycles.

Even if further investigation is needed for better establishing the nature of the redox processes exhibited by complexes **1** and **2**, the present preliminary characterization suggests that: (i) under proper experimental conditions it seems possible to isolate the Mn_8 clusters under study in different oxidation states; (ii) it seems to be easily realizable to obtain the deposition of thin films of these molecules on a substrate. This last feature is recognised as essential for the practical exploitation of SMM.

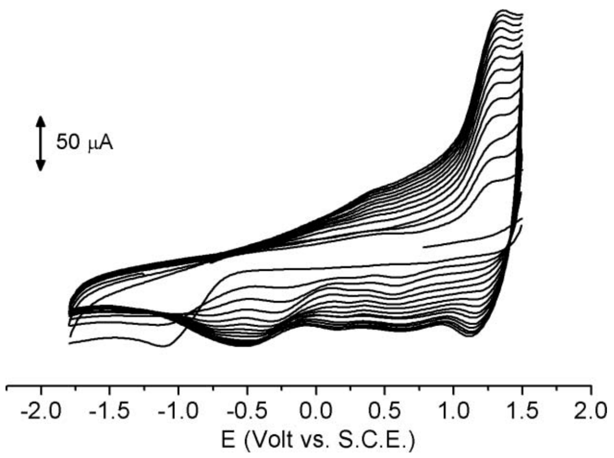

Fig. 4 Electrodeposition of a thin film of **2** at an ITO electrode in CH_2Cl_2 solution containing **2** (0.2×10^{-3} mol dm^{-3}). $[NBu_4][PF_6]$ (0.2 mol dm^{-3}) supporting electrolyte. Scan rate 0.05 V s^{-1}.

Magnetic properties

The solid-state magnetic susceptibility was measured on powdered samples in the 300–2 K range of temperature.

Susceptibility measurements were similar for the three compounds. $\chi_M T$ value decreases gradually from 16.13 (for **1**), 16.90 (for **2**) or a greater value of 20.60 cm^3 K mol^{-1} (for **3**) at 300 K down to 1.59, 1.41 or 1.25 cm^3 K mol^{-1}, respectively, at 2 K, Fig. 5. The room temperature value, lower than the expected for two Mn^{II} and six Mn^{III} non interacting ions (26.75 cm^3 K mol^{-1} for $g = 2.00$) and the constant decrease of $\chi_M T$, indicate an overall antiferromagnetic response. Magnetization measurements were also similar, showing a regular increase of the magnetization for increasing external fields, reaching non saturated values equivalent to 3.61, 3.87 or 3.89 electrons (assuming $g = 2.00$). Overparametrization excludes any reliable calculation of J coupling constants because of the large number of different interactions that relate the paramagnetic centres. Strong antiferromagnetic coupling is expected for the two pairs of Mn^{II}–Mn^{III} ions related by the alcoxo bridge with a Mn^{II}–O–Mn^{III} bond angle of 134.8°,

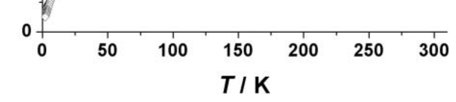

Fig. 5 Plot of the $\chi_M T$ product *vs.* T for compounds **1** (squares), **2** (solid circles) and **3** (diamonds).

leading to $S = \frac{1}{2}$ in these fragments. Moderate antiferromagnetic interactions should be expected for the interactions mediated by the μ_3 and μ_4-oxo bridges but the possibility of spin frustration in the triangles participated by Mn(1) and Mn(2) excludes any prediction of the possible spin of this fragment. However, the $\chi_M T$ values at low T strongly suggest $S = 0$ as a ground state whereas the shape of the magnetization plot show is attributable to the magnetization of the spin levels with $S > 1$ close to the ground state.

It is interesting to compare the magnetic response of **1–3** with the related malonate compound $(NB^n{}_4)_2$ [Mn_8O_4-$(O_2CPh)_{12}(Et_2mal)_2(H_2O)_2$]: the shape of the $\chi_M T$ plot is the same for all of them but the malonato compound shows a greater $\chi_M T$ value at low temperature, close to 4.5 cm^3 K mol^{-1} and the ground state was calculated to be $S = 3$. This different low T behaviour (and ground state) for so related compounds can be rationalized in basis on the Mn^{II}–O–Mn^{III} parameters involving the bdmap or malonato ligands: for the malonato ligand the Mn^{II}–O bond distance is 2.367 Å and interactions mediated by oxo bridges from carboxylate ligands are usually weak. In basis on these facts the Mn^{II}–$O_{(malonate)}$–Mn^{III} interaction was neglected by the authors and the compound treated as two weakly interacting "linked-butterfly" structure in which the spin frustrations determine the ground state. In contrast, for compounds **1–3** the stronger antiferromagnetic interaction mediated by the alcoxo Mn^{II}–$O_{(bdmap)}$–Mn^{III} bridge which is the main factor that gives a low spin ground state can not be neglected and then, the oversimplified interaction scheme applied to **4** can not be applied in our case.

Compounds **1–3** exhibit some of the conditions required for a SMM, because four of the Mn^{III} atoms (Mn(1), Mn(2) and the symmetry related) show quasi parallel elongation axis and high anisotropy should be expected from the large elongation of Mn(1) octahedron, but fails to have a large spin as ground state. The modification of these species in order to switch to a larger ground state is currently under investigation.

Conclusions

Ligands containing exclusively oxygen donors, alcoxo-pyridinic or amino di- or triols are common in Mn^{III} high nuclearity chemistry and a large number of systems with variety of nuclearities have been reported. In contrast, coordination of amminated ligands in high nuclearity clusters is extremely rare. The reported compounds give a nice example of how these type of ligands can be used to obtain large Mn^{II}/Mn^{III} clusters and how minor changes in equivalent structures can modify the ground state of this kind of compounds.

Acknowledgements

The authors thanks the Ministerio de Ciencia y Tecnología (Spain), project CTQ2009-07264, for financial support of this research and the joint project Italy-Spain (Accion Integrada 2007 in Spain, Azione Integrata 2007 in Italy) for support given to the present investigation.

References

1 Some reviews: G. Christou, D. Gatteschi, D. N. Hendrickson and R. Sessoli, *MRS Bull.*, 2000, **25**, 66; D. Gatteschi and R. Sessoli, *Angew. Chem., Int. Ed.*, 2003, **42**, 268; R. Birchner, G. Chaboussant, C. Dobe, H. Güdel, S. T. Ochsenbein, A. Sieber and O. Waldman, *Adv. Funct. Mater.*, 2006, **16**, 209; G. Aromi and E. K. Brechin, *Struct. Bonding*, 2006, **122**, 1; M. Murrie and D. J. Price, *Annu. Rep. Prog. Chem., Sect. A*, 2007, **103**, 20.

2 A. J. Tasiopoulos and S. P. Perlepes, *Dalton Trans.*, 2008, 5537.

3 E. E. Moushi, Th. C. Stamatatos, W. Wernsdorfer, V. Nastopoulos, G. Christou and A. J. Tasiopoulos, *Angew. Chem., Int. Ed.*, 2006, **45**, 7722.

4 M. Murugesu, M. Habrych, W. Wernsdorfer, K. A. Abboud and G. Christou, *J. Am. Chem. Soc.*, 2004, **126**, 4766.

5 R. T. W. Scott, S. Parsons, M. Muguresu, W. Wernsdorfer, G. Christou and E. Brechin, *Angew. Chem., Int. Ed.*, 2005, **44**, 6540.

6 D. Foguet-Albiol, T. A. O'Brien, W. Wernsdorfer, B. Moulton, M. J. Zaworotko, K. A. Abboud and G. Christou, *Angew. Chem., Int. Ed.*, 2005, **44**, 897; E. M. Rumberger, L. N. Zakharov, A. L. Rheingold and D. N. Hendrickson, *Inorg. Chem.*, 2004, **43**, 6531.

7 J. Ribas, M. Monfort, R. Costa and X. Solans, *Inorg. Chem.*, 1993, **32**, 695–699.

8 M. S. El Fallah, E. Rentschler, A. Caneschi, R. Sessoli and D. Gatteschi, *Inorg. Chem.*, 1996, **35**, 3723.

9 M. S. El Fallah, A. Escuer, R. Vicente, F. Badyine, X. Solans and M. Font-Bardia, *Inorg. Chem.*, 2004, **43**, 7218; M. S. El Fallah, F. Badyine, R. Vicente, A. Escuer, X. Solans and M. Font-Bardia, *Dalton Trans.*, 2006, 2934; M. S. El Fallah, F. Badyine, R. Vicente, A. Escuer, X. Solans and M. Font-Bardia, *Chem. Commun.*, 2006, 3113; M. S. El Fallah, R. Vicente, J. Tercero, C. Elpert, E. Rentschler, X. Solans and M. Font-Bardia, *Inorg. Chem.*, 2008, **47**, 6322.

10 P. v.d. Sluis and A.L. Spek, *Acta Crystallogr., Sect. A: Found. Crystallogr.*, 1990, **46**, 194.

11 G. M. Sheldrick, *SHELXS-97, Program for solution of crystal structures*, University of Göttingen, Germany, 1997; G. M. Sheldrick, *SHELXL-97, Program for refinement of crystal structures*, University of Göttingen, Germany, 1997.

12 M. W. Wemple, H. L. Tsai, S. Wang, J. P. Claude, W. E. Streib, J. C. Huffman, D. N. Hendrickson and G. Christou, *Inorg. Chem.*, 1996, **35**, 6437.